

Physicochemical and Analytical Studies of Some Monomer and Polymer Complexes Derived from Selected Aroyl Hydrazone

Aymen Hussien Ahmed¹, Mohsen Mahmoud Mostafa^{2*} 

¹Department of Chemistry, College of Science and Arts, Jouf University, Gurayat, Saudi Arabia

²Department of Chemistry, Faculty of Science, Mansoura University, Mansoura, Egypt

Email: *amohsenmostafa@yahoo.com

How to cite this paper: Ahmed, A.H. and Mostafa, M.M. (2022) Physicochemical and Analytical Studies of Some Monomer and Polymer Complexes Derived from Selected Aroyl Hydrazone. *Open Journal of Inorganic Chemistry*, 12, 1-17.

<https://doi.org/10.4236/ojic.2022.121001>

Received: January 2, 2022

Accepted: January 28, 2022

Published: January 31, 2022

Copyright © 2022 by author(s) and Scientific Research Publishing Inc.

This work is licensed under the Creative Commons Attribution International License (CC BY 4.0).

<http://creativecommons.org/licenses/by/4.0/>



Open Access

Abstract

New solid complexes derived from the reaction of aroyl hydrazones, 2-hydroxy-1-naphthaldehyde benzene sulphonyl hydrazone (HNB), and 2-hydroxy-1-naphthaldehyde *p*-toluene sulphonyl hydrazone (HNT), with Co²⁺, Ni²⁺, and Cu²⁺ salts have been isolated and characterized using elemental analyses, spectral (UV-vis., IR), molar conductivity and magnetic measurements. The modes of bonding as well as the stereochemistry of the isolated solid complexes were discussed. The results suggested that both HNB and HNT coordinated with the metal ions in a bidentate manner forming a polymeric chain in the case of HNB while monocular complexes were formed in the case of HNT. The amounts of solvent in the solid complexes were determined by TGA measurements. Also, spectral studies of HNT with Co²⁺ and Fe³⁺ ions in solution were carried and the ratio of complexes was determined by continuous variation, molar ratio, and slope ratio methods. Moreover, the results suggest the formation of 1:1 (M:L) for Co²⁺ ions while three species with ratios of 1:1, 1:2, and 2:1 (M:L) have been observed in the case of Ni²⁺ and Cu²⁺. Finally, conductance titration of HNB and HNT with Co²⁺ ion elucidates the formation of two species with ratios 1:1 and 1:2 (M:L) in the case of the Co²⁺-HNB while 1:1 (M:L) belongs to the Co²⁺-HNT system.

Keywords

Aroyl Hydrazones Complexes, Polymer and Monomer Complexes, FTIR, Synthesis, Stoichiometry of Complexes

1. Introduction

It is well known that hydrazones occupied a central role in the development of

coordination chemistry. This feature comes from the fact that the hydrazones, derived from the condensation of *o*-hydroxyl or methoxy aldehydes and ketones with hydrazides, are potential polynucleating ligands possessing azomethine and phenol or methoxy functions [1] offering varying bonding possibilities in metal complexes. Studies of some metal chelates of hydrazones derivatives are well known in literature [2]-[10].

On introducing the SO₂ group instead of the carbonyl group (CO) of the hydrazones moiety, the compounds are called sulphonyl hydrazones having the following formula, RSO₂NHN=CHR'. Bivalent metal complexes of benzene sulphonyl hydrazide (BS) have been studied [11]. It was reported earlier that BS coordinates to the central metal ion through the SO₂ and nitrogen of the NH group with the removal of NH proton where a polymeric chain has been suggested [12]. Moreover, salicylidene benzene sulphonyl hydrazone (HSBS) with some transition metals (M = Co²⁺, Ni²⁺, Cu²⁺, Hg²⁺, Zn²⁺, and Cd²⁺) was synthesized and characterized by different physicochemical techniques. The results showed that Ni²⁺, Cu²⁺, and Hg²⁺ form complexes with the general formula, [M(SBS)₂], while Co²⁺, Zn²⁺, and Cd²⁺ form complexes with the polymeric formula [M(SBS)₂]_n. The ligand acted in the latter case in a bidentate fashion *via* the NH and SO₂ groups (with deprotonation of the NH group forming a polymeric structure [12]).

Finally, Cu²⁺ and Ni²⁺ complexes of hydrazones derived from benzene sulphonyl hydrazine with salicylaldehyde and 2-hydroxy-1-naphthaldehyde were studied by physical and spectral methods [13]. Based on elemental analyses and spectral (i.r. and n.m.r.) data the results suggest that the isolated hydrazones behave as monobasic bidentate towards the metal cations and coordinate through the C=N and deprotonated phenol OH groups. It is worth mentioning that the spectral (Uv-vis.), magnetism as well as thermal (TG, DTG, and DTA) measurements were not been investigated for these complexes. In addition, some data obtained in this work differs from that reported before [13].

The goal of this paper is to synthesize and characterize the stereochemistry of the solid complexes derived from the reaction of 2-hydroxy-1-naphthaldehyde-benzene-sulphonylhydrazone (HNB), *p*-toluene-(HNT) with Co²⁺, Ni²⁺ and, Cu²⁺ salts. The effect of the methyl group that represents the only difference between the two synthesized hydrazones on their coordinating nature has been illustrated. Furthermore, the pK_a values of HNB and HNT were determined and the stoichiometry of complexes in solution has been determined by spectrophotometric and conductance techniques.

2. Experimental

All chemicals and solvents utilized were of BDH or AR quality and used without further purification. ¹H-NMR spectra in d₆-DMSO with TMS as internal standard were obtained from a Jeol-FX-90Q Fourier NMR spectrometer at Cairo University, Egypt. IR spectra were recorded as KBr pellet in the range "200-4000

cm^{-1} on a Mattson 5000 FTIR spectrometer at Mansoura University. Mass spectra of the ligands were performed by a Shimadzu-GC-MS-QP1000 EX using the direct inlet system at Cairo University, Egypt. Elemental analyses were determined using Perkin-Elmer 2400 at Cairo University, Egypt (Table 1). Metal contents were estimated using EDTA as reported earlier [14] [15] [16]. UV-vis. spectra of the samples in Nujol mull or DMSO, and in DMSO were measured in the range of 200 - 1000 nm using a Unicam UV2-100 spectrophotometer at Mansoura University, Egypt. The mass susceptibility of the solid complexes (χ_g) was measured with a magnetic susceptibility balance of model Sherwood at Mansoura University, Egypt. The thermal analyses (TG, DTG, and DTA) under nitrogen were carried out with a Shimadzu 50 H thermal analyzer at Mansoura University, Egypt.

2.1. Preparation of Benzene Sulphonyl Hydrazine (BH)

Benzene sulphonyl hydrazine (BH) was prepared as described earlier in the literature [11]. The isolated product was crystallized from bi-distilled water and dried in the air. A yellowish-white crystal was obtained (Mp. = 94°C).

2.2. Preparation of Hydrazones Ligands (HNB, HNT)

The two ligands, HNB and HNT, were synthesized by adding BH (0.02 mol, 3.44 g) dissolved in absolute methanol (50 mL) to a solution (50 mL) of 2-hydroxy-1-naphthaldehyde (0.02 mol, 3.44 g) (HNB) and 2-hydroxy-1-naphthaldehyde *p*-toluene sulphonyl hydrazone (HNT), respectively. The reaction mixtures were refluxed for 3 h in a water bath (95°C). The product is separated out by concentrating the solution to half of its volume and cooling. The crystals of the desired ligand were filtered off and finally recrystallized from methanol. The chemical structures of the resulting hydrazones are shown in Figure 1.

2.3. Preparation of Solid Complexes

All the isolated solid complexes (Table 1) were prepared by mixing equivocal amounts of ligands and M(II) acetates (M = Co^{2+} , Ni^{2+} , and Cu^{2+}) in 100 mL ethanol. The reaction mixture was refluxed in a water bath (95°C) for 6 h. The colored microcrystalline solids were isolated by filtration on hot, washed repeatedly

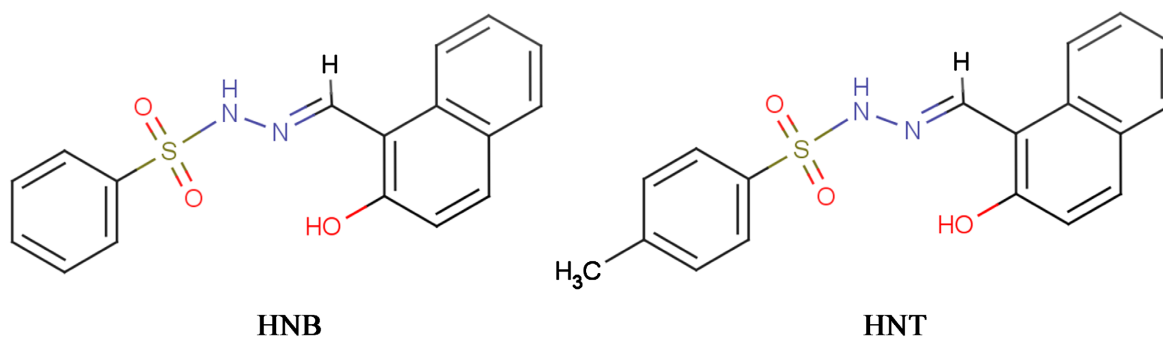


Figure 1. Chemical structures of hydrazones.

with hot ethanol, and ether, and finally dried in an oven at 80 °C for 24 h.

2.4. Preparation of Solutions for Spectrophotometric Measurements

The appropriate concentration of the metal ions (Co^{2+} and Fe^{3+}) and ligands were mixed in an absolute methanol solution. The final volume of the mixture was always kept constant by adding absolute methanol. All the absorbance measurements were recorded in the range "200 - 800 nm". Methanol was used as a blank in the case of Fe^{3+} complexes while the ligand was used as a blank in the case of Co^{2+} complexes.

3. Results and Discussion

All the analytical, physical, and spectroscopic data of the hydrazones and their isolated metal complexes are recorded in **Table 1** & **Table 2**. A comparison of the analyses for both the calculated and found percentages indicates that the composition of the isolated solid complexes coincides with the proposed formulae. All trails to isolate mono- or tris-ligand chelates by direct reaction of the ligands with the M(II) salts were unsuccessful. The complexes are air-stable for a long time, insoluble in water, alcohols, and carbon tetrachloride, and soluble in DMF and DMSO.

Table 1. Analytical, physical and spectroscopic data of the hydrazones and their complexes.

Compound	M.p. (°C), Color	Found (Calcd.)%				¹ H-NMR Chemical shift (δ ppm)**	μ_{eff}	M ⁺	Λ^*	pK _a	y
		C	H	N	M						
HNB, L ₁ C ₁₇ H ₁₄ N ₂ O ₃ S	154 Yellowish brown	63.3 (62.6)	4.2 (4.3)	8.9 (8.6)	-	11.6 (NH, s) ^a , 11.2 (OH, s) ^a , 8.85 (CH=N, s),		326 326.4		6.5	
[Cu(L ₁) ₂] _n ·nH ₂ O	206 Yellowish brown	55.9 (55.8)	4 (3.9)	-	8.2 (8.7)		1.82	-		8.1	
[Ni(L ₁) ₂ ·(EtOH) _{1/2}] _n ·2nH ₂ O	>300 Pale green	58.3 (57.4)	4.5 (4)	-	7.9 (8.0)	11.6 (NH, s) ^a , 9.0 (CH=N, s), 10.0 (EtOH, s) ^a , 6.9 - 8.2 (naphthyl and phenyl rings, m)	Diamag.	-		15.0	
[Co(L ₁) ₂] _n	>300 Brick red	57.5 (57.4)	3.7 (4)	-	8.3 (8.0)		2.34	-		18	
HNT, L ₂ C ₁₈ H ₁₆ N ₂ O ₃ S	172 Yellowish white	64 (63.5)	4.6 (4.7)	8.7 (8.2)		9.8 (NH, s), 9.4 (OH, s) ^a , 7.0 (CH=N, s), 1.4 (CH ₃ , s), 5 - 7 (naphthyl and phenyl rings, m)		340 340.4		9.5	
[Cu(L ₂) ₂ ·1/2EtOH	222 Yellowish brown	59 (58.1)	4 (4.3)	-	7.9 (8.3)		2.06	-		13	
[Ni(L ₂) ₂ ·(EtOH) _{1/2}]	291 Pale green	59.1 (58.4)	4.4 (4.4)	-	7.3 (7.7)		Diamag.	-		11	
[Co(L ₂) ₂ ·1/2EtOH·1/2H ₂ O	249 Brown	57.6 (57.7)	4.2 (4.5)	-	8.0 (7.7)		2.5	-		18	

Table 2. IR and electronic absorption data of hydrazones and their complexes.

Compound	ν (OH) phenolic	ν (NH)	ν (C=N)	ν_{as} (SO ₂)	ν_s (SO ₂)	δ (SO ₂)	δ (OH)	ν (C-O)	Solvent (EtOH/ H ₂ O)	ν M-O/ M-N	λ_{max} , nm assignments	Structure
HNB, L ₁ C ₁₇ H ₁₄ N ₂ O ₃ S	3450	3161	1620	1318	1167	574	1241	1077	-	-	366 (n- π^* , SO ₂), 354 (n- π^* , C=N), 320 ($\pi \rightarrow \pi^*$, SO ₂), 310 ($\pi \rightarrow \pi^*$, C=N), 254 ($\pi \rightarrow \pi^*$, naphthyl), 246 ($\pi \rightarrow \pi^*$, phenyl),	
[Cu(L ₁) ₂] _n ·nH ₂ O	-	3217	1615	1332	1170	576	-	1089	3300 - 3600	515/460	713 (² B ₂ → ² E), 417 (CT)	pseudo-tetrahedral
[Ni(L ₁) ₂ ·(EtOH) _{1/2}] _n ·2nH ₂ O	-	3204	1617	1329	1170	582	-	1089	3300 - 3600	520/438	620 (¹ A ₁ ' → ¹ E''), 466(¹ A ₁ ' → ¹ E'')	trigonal bipyramidal
[Co(L ₁) ₂] _n	-	3205	1616	1328	1165	585	-	1090	-	535/385	480 (² A _{1g} → ² B _{1g}), 410, 430 (CT)	square-planar
HNT, L ₂ C ₁₈ H ₁₆ N ₂ O ₃ S	3470	3196	1624	1328	1164	572	1275	1075	-	-	474 (n- π^* , SO ₂), 442 (n- π^* , C=N), 390 ($\pi \rightarrow \pi^*$, SO ₂), 366 ($\pi \rightarrow \pi^*$, C=N), 350 ($\pi \rightarrow \pi^*$, naphthyl), 336 ($\pi \rightarrow \pi^*$, phenyl)	
[Cu(L ₂) ₂ ·1/2EtOH	-	3219	1600	1330	1168	574	-	1090	3300 - 3600	515/390	716 (² B ₂ → ² E), 402 (CT)	pseudo-tetrahedral
[Ni(L ₂) ₂ ·(EtOH) _{1/2}]	-	3207	1600	1325	1168	579	-	1090	3300 - 3600	510/400	610 (¹ A ₁ ' → ¹ E''), 478(¹ A ₁ ' → ¹ E'')	trigonal-bipyramidal
[Co(L ₂) ₂ ·1/2EtOH·1/2H ₂ O	-	3208	1597	1322	1167	581	-	1089	3300 - 3600	500/410	535 (² A _{1g} → ² B _{1g})	square-planar

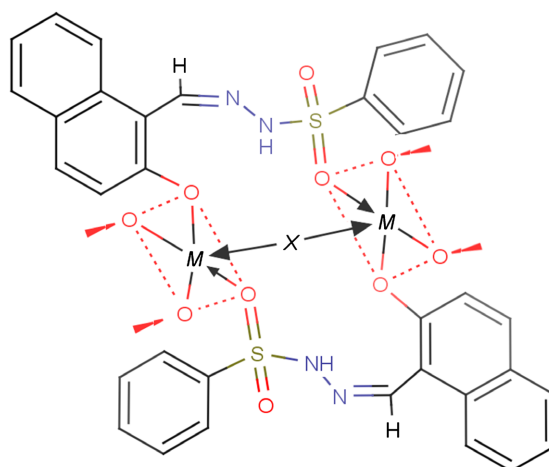
^disappeared on adding D₂O, ^b(Co-HNT system, λ_{max} = 385 nm), ^c(Fe-HNT system, λ_{max} = 530 nm), ^d(Fe-HNT system, λ_{max} = 670 nm).

3.1. IR Spectra

The positions of the IR bands of hydrazones and their metal complexes are summarized in **Table 2**. The IR spectra of HNB and HNT showed a strong band at 1620 - 1624 cm⁻¹ assigned to ν (C=N) of the azomethine. The observation of this band emphasizes the formation of the azomethine linkage. Each ligand also has a strong band in the region of 700 - 800 cm⁻¹ corresponding to the out-of-plane deformation of the aromatic rings. The observation of broad but weak bands in the 2000 - 1700 cm⁻¹ region for HNB and HNT is taken as evidence for the formation of a stable six-membered ring of intermolecular hydrogen bond of the type OH...N [17].

The IR spectral data for Co²⁺, Ni²⁺ and Cu²⁺-HNB complexes pointed out that HNB behaves as a bidentate ligand coordinating to one metal ion *via* the SO₂ and OH groups with a displacement of a proton from the latter group tending to form a polymeric chain structure (**Figure 2**). A worthy mention, it was reported that the Co²⁺ ion forms a polymeric chain with salicylidene benzene sulphony-hydrazone [12]. In fact, this suggestion is assumed on the basis of the following pieces of evidence (**Table 2**): 1) The characteristic main band of the SO₂ group at

1318 cm^{-1} assigned to $\nu_{\text{as}}(\text{SO}_2)$ shifts to a higher wavenumber by 10 - 14 cm^{-1} indicating that this group is taking part in bonding, 2) the disappearance of both $\nu(\text{OH})$ and $\delta(\text{OH})$ bands elucidates the deprotonation of this group, 3) the positive shift of $\nu(\text{C}=\text{O})$ band indicates the formation of $(-\text{C}=\text{O}-\text{M})$ bond. Nevertheless, $\text{C}=\text{N}$ was expected to involve in coordination in the case of HNB complexes, it was excluded here due to the absence of any significant shift or variation in its position or intensity upon chelating. This result is not consistent with the previously published data [12] [13]. Meanwhile, HNT coordinates in a bidentate fashion to one metal ion *via* the azomethine nitrogen ($\text{C}=\text{N}$) and OH groups (**Figure 3**). Displacement of a hydrogen proton from the latter group leads to a



$\text{M} = \text{Co}^{\text{II}}$ ($\text{X} = \text{O}$), Ni^{II} ($\text{X} = \text{EtOH}$) and Cu^{II} ($\text{X} = \text{O}$)

Figure 2. Proposed structures of the HNB complexes.

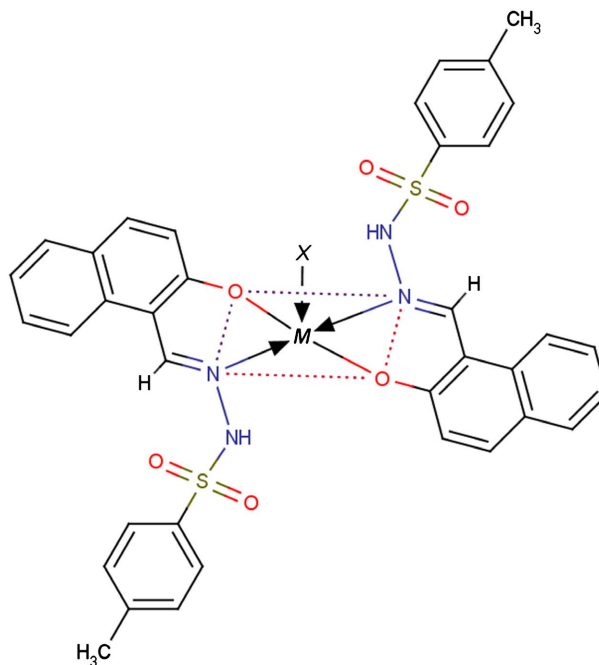


Figure 3. Proposed structures of the HNT complexes.

six-membered ring around the central metal ion. This behavior is proposed on the basis of (Table 2): 1) the characteristic three main bands of the SO₂ group at 1318, 1167 and 574 cm⁻¹ remain more or less at the same positions excluding the participation of this group in coordination, 2) the bands of both $\nu(\text{OH})$ and $\delta(\text{OH})$ vibrations disappear, and the $\nu(\text{C-O})$ band is shifting to a higher frequency, 3) the negative shift of the azomethine group to lower wavenumber confirming the involvement of this group in bonding [18]. In spite of this group is not taking part in coordination in the case of HNB which is nearly resembled in its chemical structure to HNT, it is involved here. This can be interpreted on the basis of the presence of an electron-donating group (methyl) in the *para* position for -SO₂NHN=C. This group increases the electron density on the azomethine nitrogen (N=C) of HNT (in comparison to HNB) and subsequently, its donating nature increases facilitating its linking to the metal.

Indeed, the appearance of $\nu(\text{NH})$ band with its shift to higher wavenumber in all synthesized complexes may be due to the destruction of the intermolecular hydrogen bonding between the OH and C=N groups or presumably due to the rupture of an intermolecular hydrogen bond of the type N-H.....N-H suggesting of this intermolecular H-bonding arises from the observation of $\delta(\text{NH})$ in the ¹H-NMR spectra of HNB and HNT at a higher position compared with that reported in the literature. Moreover, the persistence of new bands in the IR spectra of metal complexes as shown in Table 2 assigned to M-O and/or M-N indicates the formation of the metal complexes. The observation of only one band for each Co-N and Co-O group suggests the existence of trans-configuration [19]. Strong broad absorption in the 3300 - 3600 cm⁻¹ region for metal complexes substantiates the presence of water and/or ethanol.

3.2. ¹H-NMR Spectra

The assignments of the main signals in ¹H-NMR spectra of the ligands under investigation are shown in Table 1. ¹H-NMR spectra of hydrazones exhibit three signals with equal integration (1:1:1) at (11.59, 11.2, 8.85) and (9.8, 9.4, 7.0) ppm, downfield of TMS, and assigned to the protons of (NH, OH, CH=N) of HNB and HNT, respectively. On adding two drops of D₂O, the NH and OH signals disappeared while the signal of CH=N remained. The higher frequency of the OH signal(s) compared with that reported in the literature is most probably due to the intermolecular hydrogen bonding operating between the hydrogen atom of the *ortho*-hydroxyl group and the azomethine nitrogen (OH...N-type) as previously confirmed by the IR data. By comparing the ¹H-NMR spectra of HNB (HL₁) with its relating Ni(II) complex namely, [Ni(L₁)₂(EtOH)_{1/2}].2H₂O, it is evident that 1) no signal is recorded for a phenol hydroxyl proton at 11.2 ppm, as in case of the HNB hydrazones indicating deprotonation of the *ortho*-hydroxy group 2) the remaining of the signals attributed to the proton of NH and CH=N groups at nearly the same positions (Table 1) confirms the un participation of these groups in coordination and thus coincides with the obtained IR data and

the proposed polymeric chain structure [20]. Perhaps, this comparison explains the coordination behavior of HNB with Co^{2+} and Cu^{2+} salts which are analogous complexes. It is well known that Co^{2+} , Ni^{2+} , and Cu^{2+} ions are resembled in their chemical behavior due to the convergence in their ionic radii.

3.3. Electronic and Magnetic Spectra

The electronic spectra of the hydrazones and their solid metal complexes [21] [22] [23] [24] as well as the geometry and magnetic data of the formed chelates are shown in **Table 2**. The redshift of HNT bands in comparison to that observed in the case of HNB (**Table 2**) is mainly due to the existence of the methyl group in the para-position. This electron-donating group increases the electron density on the $\text{O}=\text{S}=\text{O}$, $\text{C}=\text{N}$, and OH groups, and consequently, a redshift was observed. The electronic spectra of the metal chelate suggest different environments around the metal ions. The results revealed that Cu^{2+} complexes are pseudo-tetrahedral; Ni^{II} complexes are trigonal-bipyramidal while Co^{2+} complexes have square-planar geometry. For the magnetic studies, the values of μ_{eff} of all complexes may be considered in good agreement with the proposed structures [25] [26] [27].

3.4. Thermal Analysis

The thermal decomposition studies (TG, DTG, and/or DTA) on major solid metal complexes have been carried out. The TG curves up to 800°C for complexes showed 3-5 stages of decompositions with the formation of metal carbonates/oxides/carbide or mixtures of them at the last stage. The results of the thermal analysis revealed that: 1) $[\text{Co}(\text{L}_1)_2]_n$ showed a first weight-loss stage at 219°C assignable to the decomposition of the complex and at the same time emphasized the absence of any crystalline solvent. This temperature (219°C) is high enough to be considered for out sphere ethanol or water. The TG curve is ended by the existence of CoCO_3 , 2) $[\text{Co}(\text{L}_2)_2] \cdot 1/2\text{EtOH} \cdot 1/2\text{H}_2\text{O}$ decomposed at 275°C and ended by CoCO_3 as well. The two weak bands in the range 100°C - 200°C suggest the removal of the solvent ($1/2\text{EtOH} + 1/2\text{H}_2\text{O}$), 3) $[\text{Ni}(\text{L}_1)_2(\text{EtOH})_{1/2}]_n \cdot 2n\text{H}_2\text{O}$ and $[\text{Ni}(\text{L}_2)_2(\text{EtOH})_{1/2}]$ decomposed at 134 and 322°C , respectively. The residue corresponds to the formation of nickel carbonate, oxide, and carbide. The first weight-loss stage at 74°C in case of $[\text{Ni}(\text{L}_1)_2(\text{EtOH})_{1/2}]_n \cdot 2n\text{H}_2\text{O}$ corresponds to the removal of $1/2\text{EtOH} + 2\text{H}_2\text{O}$ while the DTA diagram for $[\text{Ni}(\text{L}_2)_2(\text{EtOH})_{1/2}]$ showed an endothermic peak at 90°C corresponding to the removal of $1/2\text{EtOH}$ molecule from the complex, 4) TG curve of $[\text{Cu}(\text{L}_2)_2] \cdot 1/2\text{EtOH}$ showed a first decomposition stage at 216°C . This stage is accompanied by an exothermic peak in the DTA curve indicating the starting of decomposition. On the other hand, the DTA showed an endothermic peak at 102°C assignable to the removal of $1/2\text{EtOH}$.

In the light of the foregoing results, the most reasonable structures of the $\text{M}(\text{II})$ chelates can be represented by **Figure 2** and **Figure 3**, respectively.

The behavior of Co^{2+} and Fe^{3+} ions with HNT has been studied and the stoichiometry was determined. The other ligand under investigation (HNB) is not investigated since it precipitates a solid complex with Co^{2+} and gives unspecified color with Ni^{2+} and Cu^{2+} ions (*i.e.*, a mixed color of HNB and metal (II) ion without any reaction).

3.5. Spectral Studies in Solution

Comparing the spectra of the Co^{2+} , and Fe^{3+} -HNT complexes with HNT and the employed metal salt solutions (cobalt acetate and ferric chloride) at room temperature showed a new band at 385 nm with a shoulder at 400 nm for Co^{2+} -HNT and a band at 670 nm in case of Fe^{3+} -HNT. Increasing the concentration of the ligand (from 1×10^{-4} to 1×10^{-4} M for Co^{2+} -HNT and to 6×10^{-4} M for Fe^{3+} -HNT) leads to a hyperchromic shift without changing the position of the band manifesting the formation and stabilization of the complex in solution. On leaving Fe^{2+} -HNT solution for 42 h, it was noticed that the color of the solution has been changed from green to brown accompanied by a hypsochromic shift for the absorption maxima from λ_{max} at 670 nm (green solution) to 530 nm (brown solution). This indicates that the Fe^{3+} complex formed at once is quite stable but attains maximum stability after 42 h. Besides, it suggests the increase of 10 Dq, and consequently, the geometry of the complex may be changed. From this view, the effect of temperature on a Fe^{3+} -HNT is of considerable interest to be studied. Increasing the temperature from 25 to 55 °C for the Fe^{3+} -HNT system reveals a hypsochromic shift for λ_{max} from 670 to 560 nm (**Figure 4**). Doubtless, this indicates that the increase of temperature helps too much for reaching the stability of the formed complex.

To trace the complex formation and deduce the stoichiometry of the complexes in solution, continuous variation [28], the molar ratio [29], and slope ratio [30] methods were employed. For the Co^{2+} -HNT mixture, the results obtained (at $\lambda_{\text{max}} = 385$ nm) by continuous variation (**Figure 5**), molar ratio, and slope ratio indicated the formation of the complex with 1:1 (Co^{2+} : HNT). On the

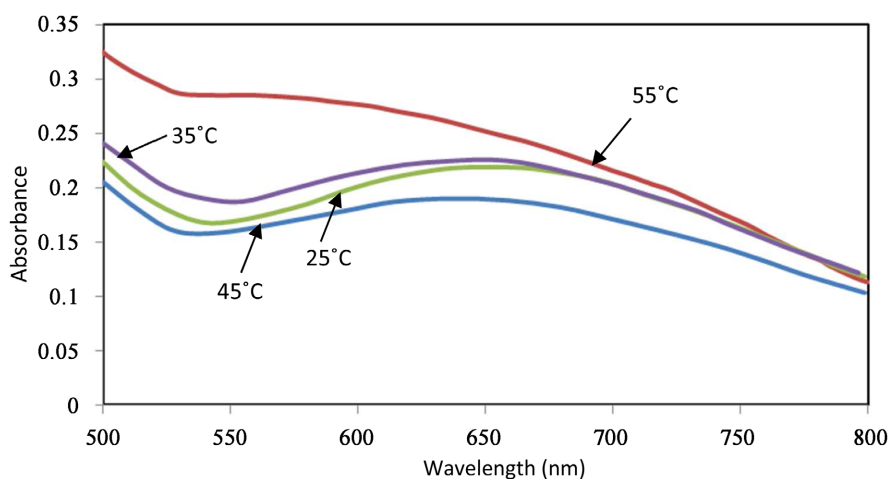


Figure 4. Effect of temperature on FeCl_3 -HNT complex.

other hand, the results of continuous variation, molar ratio, and slope ratio methods for Fe^{3+} -HNT mixture at the λ_{max} 's = 670 and 530 nm at once and after 42 h are in good agreement with each other and manifested the existence of 1:2 (Fe^{3+} :HNT) and 2:1 (Fe^{3+} :HNT) complexes, respectively. The continuous variation diagram (Figure 6, and Figure 7) revealed also a 1:1 (Fe^{3+} :HNT) species at 530 nm, and high intensity for 2:1 (Fe^{3+} :HNT) compared with 1:1 and 1:2 (Fe^{3+} :HNT) indicating the higher stability of the 2:1 M:L complex. Based on the obtained results, it is suggested that 1:2 (Fe^{3+} :HNT) was reached to 2:1 (Fe^{3+} :HNT) passing by 1:1 (Fe^{3+} :HNT). Also, It is very conspicuous that the stability of the 2:1 (Fe^{3+} :HNT) complex increases with time and temperature. A literature survey pointed out that the octahedral FeF_3^{3-} showed a band at 704 nm while the tetrahedral FeBr_4^- showed a band at 588 nm [31]. According to this fact, the hypsochromic shift of λ_{max} from 670 to 530 nm may be due to two probabilities (1) the geometry of the Fe^{3+} -HNT complex was changed from octahedral to tetrahedral due to the steric effect of ligand or (2). The kind of ligands was varied

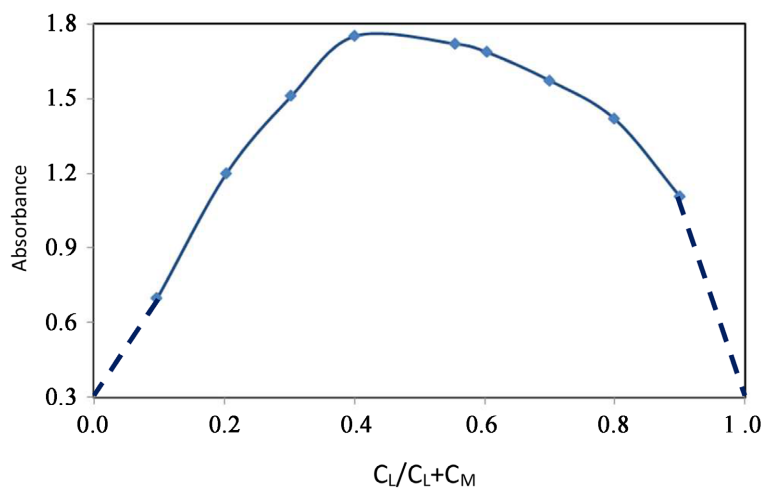


Figure 5. Continuous variation method for Co(II)-HNT complex.

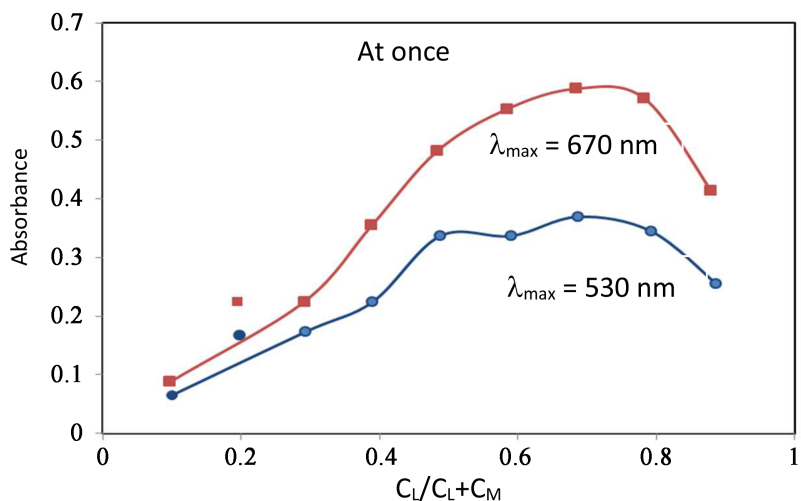


Figure 6. Continuous variation method for Co(II)-HNT complex.

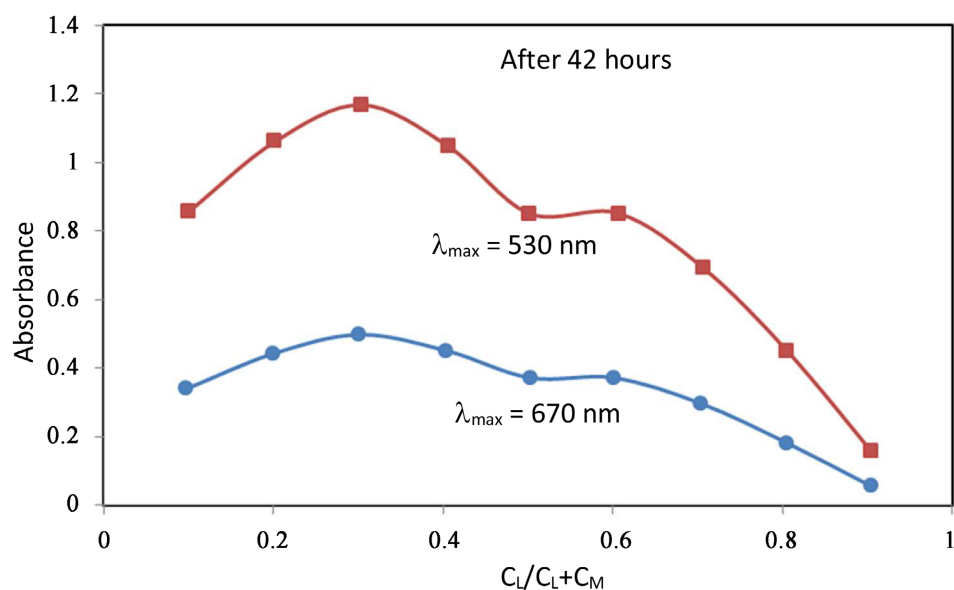


Figure 7. Continuous variation method after 42h for FeCl_3 -HNT complex.

but with preservation of the geometry *i.e.*, the electronic field strength of ligands increased.

Spectrophotometric studies on the complexation of Co^{2+} and Fe^{3+} with HNT were performed in order to show the possibility of applying the reaction for the micro-determination of those two metal ions. Both Co^{2+} and Fe^{3+} ions are only selected within the all investigated metal ions since they exhibit a change in color which can be detected in the visible region. For this purpose, absorbance measurements were carried out by adding the metal salt solution in varying concentrations to a constant concentration of HNT in absolute MeOH. On plotting the obtained absorbance values at the above selected wavelengths (385, 670, and 530 nm) against the corresponding concentration of the metal ions to verify Beer's law, linear relations were obtained (calibration curve). At a higher concentration of M^{n+} , a negative deviation was observed. The results suggested that Beer's law is obeyed for 1) Co^{2+} -HNT system at $\lambda_{\text{max}} = 385$ nm up to 0.1×10^{-3} M, 2) Fe^{3+} -HNT (at once and RT) at, $\lambda_{\text{max's}} = 530$ and 670 nm up to 0.5×10^{-3} M and 3) Fe^{3+} -HNT (after 42 h) at, $\lambda_{\text{max's}} = 530$ and 670 nm up to 2×10^{-3} M. The sensitivity y values (Table 1) were estimated by Sandall's method [32] following the equations:

$$y = n(\text{at.wt})/\varepsilon$$

$$\varepsilon = A/bc$$

where:

y = sensitivity (number of micrograms of an element present as the absorbing species in a column solution of 1 cm^2 cross-section giving an absorbency of 0.001 at specified wavelength).

n = number of elements in a molecule of the compound.

At.wt = atomic weight of the element in gram.

ε = molar absorptivity.

A = maximum absorbance obeyed Beer's law.

c = concentration corresponding to the absorbance A .

b = thickness of the utilized quartz cell (1 cm).

3.6. Effect of pH on the Absorption Spectra of HNT and HNB

Absorption spectra of HNT (1×10^{-4} M) and HNB (1.2×10^{-5} M) in universal buffer solutions were recorded in the range of 200 - 450 nm. The spectra exhibit one band in the pH range 8 - 12 at 353 and 243 nm for HNB and HNT, respectively. No absorbance was traced in the lower pHs (1 - 7) in the case of HNB owing to the participation that occurred. The relation between absorbance versus the pH was represented in **Figure 8** and **Figure 9** shows the S-shape curve. The pK_a values were calculated from these curves and located in **Table 1**. The

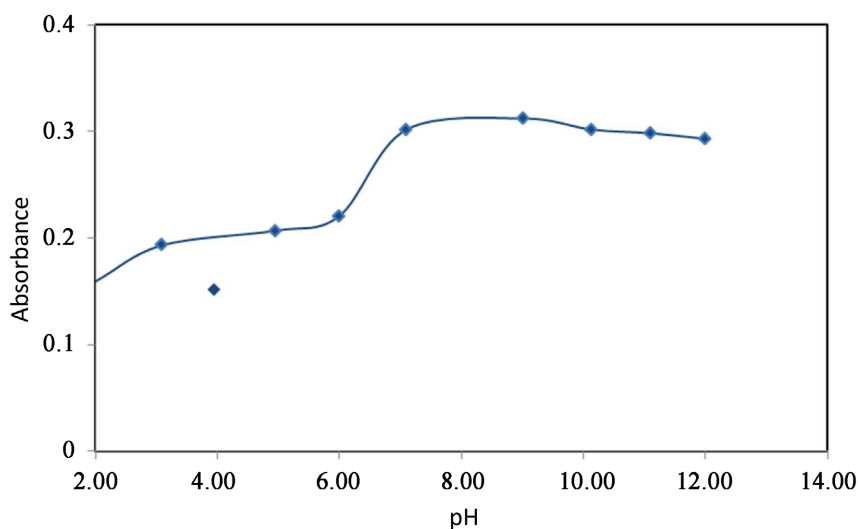


Figure 8. Effect of universal buffer on HNB ligand.

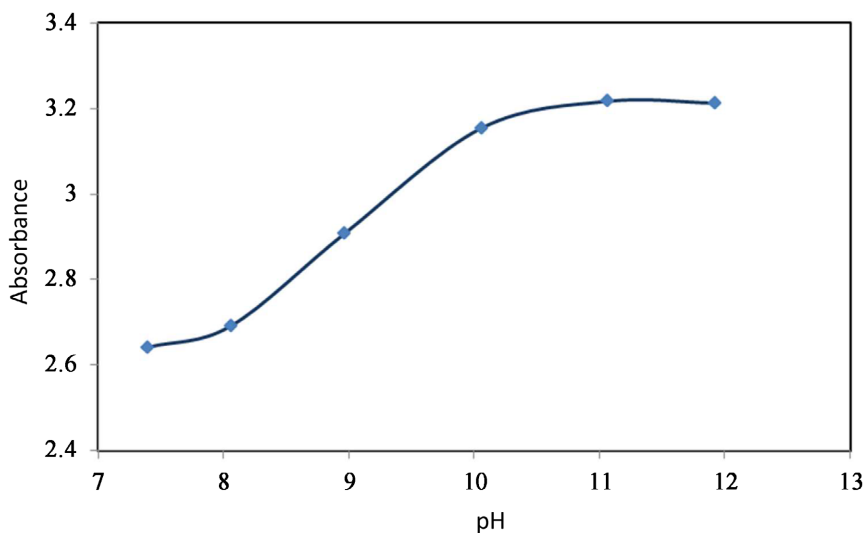


Figure 9. Effect of universal buffer on HNT ligand.

smaller pK_a value of HNB (6.5) compared with that of HNT (9.5) arises from the effect of the electron-donating nature of the (CH_3) group in HNT which increases the electron density on the OH (naphthyl) group and consequently, the pK_a was observed at high pH value. On the other hand, the existence of a withdrawing group (phenyl) in HNB decreases the electron density on the OH (naphthyl) group and hence the pK_a has a small value.

Utilizing absolute methanol solutions, conductance titration of 10 mL (2.5×10^{-4} M) cobalt acetate solution with HNB (2.5×10^{-3} M) and 25 mL of cobalt acetate solution (5×10^{-4} M) with HNT (5×10^{-3} M) were carried out and represented in **Figure 10** and **Figure 11**, respectively. The results of the Co^{2+} -HNB curve (**Figure 10**) showed two breaks at 1:1 and 1:2 (Co^{2+} :HNB). This illustrates that the two complex species with different ratios are possibly formed

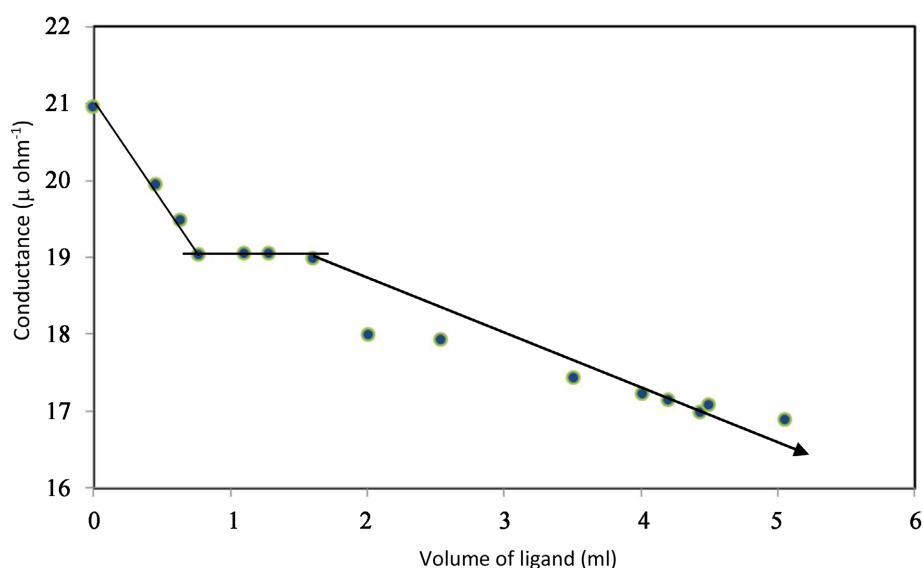


Figure 10. Conductometric titration for $Co(OAc)_2$ -HNB system.

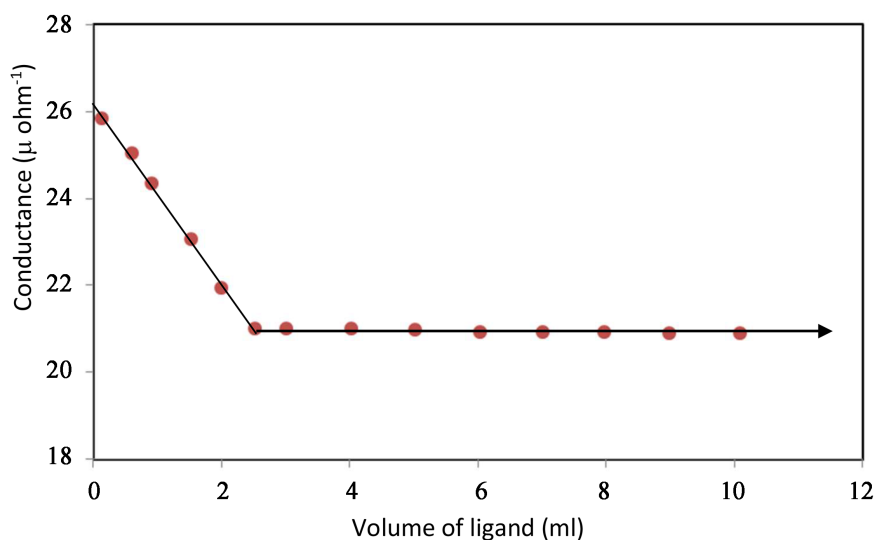


Figure 11. Conductometric titration for $Co(OAc)_2$ -HNT system.

in solution and hence we could obtain each of them by adding the appropriate amount of the ligand. Fe³⁺-HNB curve (**Figure 11**) revealed only one break at 1:2 (Co²⁺:HNT).

A common behavior of these curves is the continuous decrease of the reaction mixture conductance with increasing the number of hydrazones added. This suggests the formation of non-electrolytic species in solution, *i.e.*, the reaction of HNB or HNT with Co²⁺ acetate proceeds without the liberation of acetic acid. Conversely, Co²⁺-HNB, HNT complexes were isolated as solids by deprotonation of ligand and thus the acetic acid was liberated. This can be interpreted on the basis of various reaction conditions. To explain this contrariety, we proposed that HNB or HNT reacts with cobalt acetate in solution and at room temperature forming an octahedral geometry around the Co²⁺ ion. Upon refluxing the reaction mixture, the liberation of acetic acid is induced and finally, a non-electrolytic complex species having a square-planar geometry is obtained as in the solid-state. This mechanism can be shown in case of HNB ligand as follow:



The same mechanism is proposed for the Co²⁺-HNT complex. Finally, the molar conductivity of all complexes is shown in **Table 1**. The values indicate a non-electrolytic nature in this solvent and are consistent with the other results.

4. Conclusion

The results obtained in this work verified that a number of aroyl hydrazones complexes, derived from 2-hydroxy-1-naphthaldehyde, have been successfully synthesized. The compositions and structures of these complexes have been established on the basis of different physicochemical techniques. The mode of binding of the aroyl hydrazones under investigation mainly depends on the substitute in the *para*-position of the phenyl ring. The persistence of the electron-donating group in the *para*-position of phenyl ring *e.g.*, methyl group increases the electron density on azomethine nitrogen and consequently facilitates its coordination with the metal cation. This is very conspicuous in the solid complexes of aroyl hydrazones with cobalt, nickel, and copper ions. The chelating takes place with the replacement of phenol hydrogen along with the linking of an auxiliary group that is SO₂ in HNB and C=N in HNT forming complexes with a ratio of 1:2 (M: L) composition for HNB and polymer chains with HNT. Spectrophotometric and conductance titration studies can be used to identify the stoichiometry of the aroyl hydrazones with some metal cations and the former technique substantiates the possibility of micro determination of Co²⁺ and Fe³⁺ ions by the aroyl hydrazones.

Conflicts of Interest

The authors declare no conflicts of interest regarding the publication of this paper.

References

- [1] Abdulghani, A.J. and Abbas, N.M. (2011) Synthesis Characterization and Biological Activity Study of New Schiff and Mannich Bases and Some Metal Complexes Derived from Isatin and Dithiooxamide. *Bioinorganic Chemistry and Applications*, **2011**, Article ID: 706262. <https://doi.org/10.1155/2011/706262>
- [2] Despaigne, A.A.R., Da Silva J.G., Do Carmo, A.C.M., Piro, O.E., Castellano, E.E. and Beraldo, H. (2009) Copper(II) and Zinc(II) Complexes with 2-Benzoylpyridine-Methyl Hydrazine. *Journal of Molecular Structure*, **920**, 97-102. <https://doi.org/10.1016/j.molstruc.2008.10.025>
- [3] Raj, B.N.B., Kurup, M.R.P. and Suresh, E. (2008) Synthesis, Spectral Characterization and Crystal Structure of *N*-2-Hydroxy-4-Methoxybenzaldehyde-*N'*-4-Nitrobenzoyl Hydrazone and Its Square Planar Cu(II) Complex. *Spectrochimica Acta Part A: Molecular and Biomolecular Spectroscopy*, **71**, 1253-1260. <https://doi.org/10.1016/j.saa.2008.03.025>
- [4] Abouel-Enein, S., El-Saied, F.A., Emam, S.M. and Ell-Salamony, M.A. (2008) First Row Transition Metal Complexes of Salicylidene and 2-Hydroxy-1-Naphthylidene-*N*-Cyanoacetohydrazone. *Spectrochimica Acta Part A: Molecular and Biomolecular Spectroscopy*, **71**, 421-429. <https://doi.org/10.1016/j.saa.2007.12.031>
- [5] Pedrares, A.S. Camiña, N., Romero, J., Durán, M.L., Vázquez, J.A.G. and Sousa, A. (2008) Electrochemical Synthesis and Crystal Structure of Cobalt(II), Nickel(II), Copper(II), Zinc(II) and Cadmium(II) Complexes with 2-Pyridinecarbaldehyde-(2-Aminosulfonylbenzoyl) Hydrazone. *Polyhedron*, **27**, 3391-3397. <https://doi.org/10.1016/j.poly.2008.08.011>
- [6] Chandra, S. and Sharma, A.K. (2009) Ni(II) and Cu(II) Complexes with Base Ligand 2,6-Diascetylpyridine Bis-(Arbohydrazone): Synthesis and I.R. Mass ¹HNMR Electronic and EPR. *Spectrochimica Acta Part A: Molecular and Biomolecular Spectroscopy*, **72**, 851-857. <https://doi.org/10.1016/j.saa.2008.12.022>
- [7] Yacoute-Nour, A., Mostafa, M.M. and Maki, A.K.T. (1990) New Uranyl(VI) Complexes with Hydrazones Derived from Aliphatic and Aromatic Acid Hydrazides Containing Dihydroxo Bridges. *Transition Metal Chemistry*, **15**, 34-38. <https://doi.org/10.1007/BF01032228>
- [8] El-Shazely, R.M., Souliman, M.S. Shallby, A.M. and Mostafa, M.M. (1990) Synthesis of New Metal Complexes Derived from Cyanocetylhydrazone (SCH) and Its Derivatives with Some Transition Metal Ions in Isopropanol and Tert-Butanol. (IV). *Synthesis and Reactivity in Inorganic and Metal-Organic Chemistry*, **20**, 301-318. <https://doi.org/10.1080/00945719008048136>
- [9] Souliman, M.S., Shallaby, A.M., El-Shazely, R.M. and Mostafa, M.M. (1987) Reactions of Cyanoacetylhydrazine Complexes with Salicylaldehyde and Consequent Metal-Promoted Reactions. *Polyhedron*, **6**, 1319-1323. [https://doi.org/10.1016/S0277-5387\(00\)80889-X](https://doi.org/10.1016/S0277-5387(00)80889-X)
- [10] Mondal, B., Drew, M.G.B. and Ghosh, T. (2009) Synthesis, Structure and Solution Chemistry of Quaternary Oxovanadium(V) Complexes Incorporating Hydrazone Ligands. *Inorganica Chimica Acta*, **362**, 3303-3308. <https://doi.org/10.1016/j.ica.2009.02.043>
- [11] Rakha, T.H., El-Asmy, A.A., Mostafa, M.M. and El-Kourshy, A. (1987) Synthesis and Structural Studies on Bivalent Benzene Sulphonylhydrazine. *Transition Metal Chemistry*, **12**, 125-127. <https://doi.org/10.1007/BF01022337>
- [12] Larabi, L. Harek, Y., Reguig, A. and Mostafa, M.M. (2003) Synthesis, Structural Study and Electrochemical Properties of Copper(II) Complexes Derived from Ben-

- zene- and *p*-Toluenesulphonylhydrazones. *Journal of the Serbian Chemical Society*, **68**, 85-95. <https://doi.org/10.2298/ISC0302085L>
- [13] Shawali, A.S., Aboutabl, M.A., Fahmy, H.M., Mazza, A., Osei-Twum, E.Y. and Abbas, N.M. (1992) Chelate Formation by Hydrazones. *Transition Metal Chemistry*, **17**, 517-520. <https://doi.org/10.1007/BF02910747>
- [14] Vogel, A.I. (1989) A Text Book of Quantitative Inorganic Analysis. 5th Edition, Longmans, London.
- [15] Ahmed, A.H., Omran, A.A. and El-Sherbiny, G.M. (2007) Synthesis, Characterization and Biological Evaluation of Some Methylene Salicylic Acid Complexes. *Journal of Applied Sciences Research*, **2**, 44-50.
- [16] Ali, A.M., Ahmed, A.H., Mohamed, T.A. and Mohamed, B.H. (2007) Chelates and Corrosion Inhibition of Newly Synthesized Schiff Bases Derived from *o*-Toluidine. *Transition Metal Chemistry*, **32**, 461-467. <https://doi.org/10.1007/s11243-007-0184-8>
- [17] Shallaby, A.M., Mostafa, M.M., Ibrahim, K.M. and Moussa M.N.H. (1984) New Uranyl(VI) Complexes with Hydrazone-Oximes Derived from Aromatic Acid Hydrazides and Biacetylmonoxime-I. *Spectrochimica Acta Part A: Molecular and Biomolecular Spectroscopy*, **40**, 999-1002. [https://doi.org/10.1016/0584-8539\(84\)80160-9](https://doi.org/10.1016/0584-8539(84)80160-9)
- [18] Osunlaja, A.A., Ndahi, N.P. and Ameh J.A. (2009) Some Synthesis, Physico-Chemical and Antimicrobial Properties of Co(II), Ni(II) and Cu(II) Mixed-Ligand Complexes of Dimethylglyoxime—Part I. *African Journal of Biotechnology*, **8**, 4-11.
- [19] Ferraro, J.R. (1971) Low-Frequency Vibration of Inorganic and Coordination Compounds. Springer, New York. <https://doi.org/10.1007/978-1-4684-1809-5>
- [20] Jeewoth, T., Bhowon, M.G. and Wah, H.L. (1999) Synthesis, Characterization and Antibacterial Properties of Schiff Bases and Schiff Base Metal Complexes Derived from 2,3-Diamino-Pyridine. *Transition Metal Chemistry*, **24**, 445-448.
- [21] Sutton, D. (1968) Electronic Spectra of Transition Metal Complexes. McGraw Hill, London
- [22] Dien, L.X., Truong, N.X., Yamashita, K. and Sugiura, K. (2020) Metal Complexes of π -Expanded Ligands (4): Synthesis and Characterizations of Copper(II) Complexes with a Schiff Base Ligand Derived from Pyrene. *VNU Journal of Science. Natural Sciences and Technology*, **36**, 62-72. <https://doi.org/10.25073/2588-1140/vnunst.4983>
- [23] Bai, B., Wang, D. and Wan, L. (2021) Synthesis of Covalent Organic Framework Films at Interface. *Bulletin of the Chemical Society of Japan*, **94**, 1090-1098. <https://doi.org/10.1246/bcsj.20200391>
- [24] Morassi, R.I. Bertini, G. and Sacconi, L. (1972) Five-Coordination in Iron(II); Cobalt(II) and Nickel(II) Complexes. *Coordination Chemistry Reviews*, **11**, 343-402. [https://doi.org/10.1016/S0010-8545\(00\)80248-9](https://doi.org/10.1016/S0010-8545(00)80248-9)
- [25] Cotton, F.A. and Wilkinson, G. (1999) Advanced Inorganic Chemistry. Interscience, New York.
- [26] Lever (1965) The Magnetic Moments of Some Tetragonal Nickel Complexes. *Inorganic Chemistry*, **4**, 763-764. <https://doi.org/10.1021/ic50027a041>
- [27] Morassi, R. and Dei, A. (1972) The Solution Behavior of Nickel(II) Halide Complexes of 1,2-Bis(Diphenylphosphino)Ethane (dpe): The Existence of Five-Coordinate $[\text{Ni}(\text{dpe})_2\text{X}]^+$ Species. *Inorganica Chimica Acta*, **6**, 314-316. [https://doi.org/10.1016/S0020-1693\(00\)91805-X](https://doi.org/10.1016/S0020-1693(00)91805-X)

-
- [28] Renny J. S, Tomasevich L.L., Tallmadge. E.H. and Collum, D.B. (2013) Method of Continuous Variations: Applications of Job Plots to the Study of Molecular Associations in Organometallic Chemistry. *Angewandte Chemie International Edition*, **11**, 11998-12013. <https://doi.org/10.1002/anie.201304157>
- [29] Yoe, G.H. and Jones, A.L. (2021) Spectrophotometric Investigation of Complexation of Ferrous Ion with 3,5-Dinitrosalicylic Acid. *World Journal of Chemical Education*, **9**, 77-80. <https://doi.org/10.12691/wjce-9-3-2>
- [30] Divarova, V.V., Lekova, V.D., Racheva, P.V., Stojnova, T.K., and Dimitrov A.N. (2014) Ternary Ion-Association Complexes of Cobalt with 4-(2-pyridylazo) Resorcinol and Tetrazolium Salts. *Acta Chimica Slovenica*, **61**, 813-818.
- [31] Lever, A.B.P. (1963) *Inorganic Electronic Spectroscopy*. Elsevier Publishing Company, Amsterdam
- [32] Sandell, E.B. and Onishi, H. (1978) *Photometric Determination of Traces of Metals General Aspects of Metals*. John Wiley, New York.